

10

12

THE EFFECT OF THE GROUND PLANE ON
LOW ASPECT RATIO SWEEP WINGS

A THESIS

Presented to
the Faculty of the Graduate Division
Georgia Institute of Technology

In Partial Fulfillment
of the Requirements for the Degree
Master of Science in Aeronautical Engineering

By

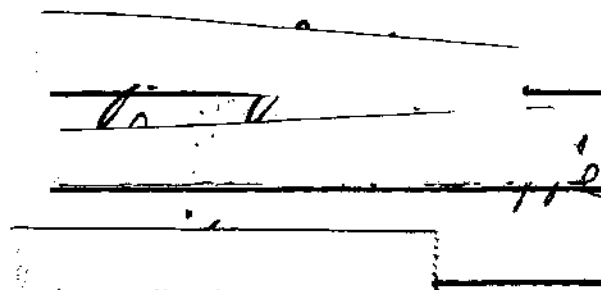
Sidney Alan Powers

February 1955

In presenting the dissertation as a partial fulfillment of the requirements for an advanced degree from the Georgia Institute of Technology, I agree that the Library of the Institution shall make it available for inspection and circulation in accordance with its regulations governing materials of this type. I agree that permission to copy from, or to publish from, this dissertation may be granted by the professor under whose direction it was written, or, in his absence, by the Dean of the Graduate Division when such copying or publication is solely for scholarly purposes and does not involve potential financial gain. It is understood that any copying from, or publication of, this dissertation which involves potential financial gain will not be allowed without written permission.

THE EFFECT ON THE GROUND PLANE ON
LOW ASPECT RATIO SWEEP WINGS

Approved:



The signature area contains several horizontal lines. The top line is a solid line. Below it is a line with some handwritten scribbles. The next line is another solid line. Below that is a line with a small mark on the right side. The bottom line is a solid line.

Date Approved by Chairman: Feb 9, 1955

ACKNOWLEDGEMENTS

The author wishes to express his appreciation to Professor J. J. Harper who first proposed the topic and acted as advisor, and to Professor A. L. Ducoffe who provided much valuable criticism. The author is also indebted to Professor D. W. Dutton and the entire Aeronautical Engineering staff and the Georgia Institute of Technology for their valuable assistance and financial aid, without which this thesis could not have been compiled. Gratitude is also extended to Professor M. J. Goglia for his review of the topic.

LIST OF SYMBOLS

a	constant
A	aspect ratio, b^2/S
b	wing span
B	coefficient defining the change in circulation
c	chord length
c_l	local, or two dimension lift coefficient
C_L	wing lift coefficient, Lift/qS
D	coefficient defining the change in moment due to the image wing
e	wing thickness in chord lengths, t/c
E	coefficient defining the change in Moment due to wing thickness
K	coefficient defining the change in angle of attack due to wing thickness
H	height of the quarter chord point of the wing Mean Aerodynamic Chord above the ground
MAC	Mean Aerodynamic Chord of the wing
n	arbitrary reduction factor for the lift curve slope
q	dynamic pressure, $0.5\rho V^2$
r	reduction factor to account for the finite wing
S	wing area
T	coefficient defining the change in velocity due to the image wing
v	increase in velocity
V	free stream velocity
α	angle of attack

β	change in circulation
γ	local vortex strength on vortex sheet
K	change in effective angle of attack due to wing thickness
ξ	position on vortex sheet
ρ	density
σ	Prandtl's biplane interference factor
τ	change in velocity due to image wing

TABLE OF CONTENTS

	Page
ACKNOWLEDGEMENTS	ii
LIST OF SYMBOLS	iii
LIST OF FIGURES	vi
SUMMARY	viii
 Chapter	
I. INTRODUCTION	1
II. THEORETICAL ANALYSIS OF THE PROBLEM	2
III. MODELS AND EQUIPMENT	8
IV. PROCEDURE	10
V. RESULTS	12
VI. CONCLUSIONS	19
VII. RECOMMENDATIONS	20
APPENDIX	21
BIBLIOGRAPHY	43

LIST OF FIGURES

Figure	Page
1. Definition of Equation 18	7
2. Dimensions of Delta Wing Model	21
3. Dimensions of Straight Wing Model	22
4. Ground Plane Positions	23
5. Straight Wing and High Ground Plane	24
6. Delta Wing and Mid Ground Plane	24
7. Lift Curves for Delta Wing	25
8. Drag Polars for Delta Wing	26
9. Pitching Moment Curves for Delta Wing	27
10. Lift Curves for Straight Wing	28
11. Drag Polars for Straight Wing	29
12. Pitching Moment Curves for Straight Wing	30
13. Delta Wing Tuft Study, $\alpha = 5.0^\circ$	31
14. Delta Wing Tuft Study, $\alpha = 10.3^\circ$	32
15. Delta Wing Tuft Study, $\alpha = 15.6^\circ$	33
16. Delta Wing Tuft Study, $\alpha = 21.0^\circ$	34
17. Delta Wing Tuft Study, $\alpha = 26.3^\circ$	35
18. Straight Wing Tuft Study, $\alpha = 0^\circ$	36
19. Straight Wing Tuft Study, $\alpha = 8.0^\circ$	36
20. Straight Wing Tuft Study, $\alpha = 16.0^\circ$	37
21. Straight Wing Tuft Study, $\alpha = 17.0^\circ$	37

Figure	Page
22. Span Loading for Delta	38
23. Incremental Ground Effects, Angle of Attack	39
24. Incremental Ground Effects, Drag	40
25. Incremental Ground Effects, Pitching Moment	41
26. Incremental Ground Effects on 40° Swept Wing	42

SUMMARY

Two wings of aspect ratio 1.732, one straight and one swept, were tested in the nine foot wind tunnel of the Daniel Guggenheim School of Aeronautics to determine the effect of ground proximity on the aerodynamic characteristics of such wings. Each wing was tested at three heights above the ground plane, and with no ground plane.

It was found that the effect of the ground was greater on the swept wing than on the straight wing, for the same height to semi-span ratio, $\frac{2H}{b}$. In general, for a given lift coefficient the angle of attack is reduced, the drag coefficient is reduced, and the pitching moment coefficient is made more negative by the presence of the ground.

An analytic method that was applied underestimated the changes in the aerodynamic characteristics for the swept wing, but provided acceptable preliminary lift drag data for the straight wing.

CHAPTER I

INTRODUCTION

The addition of a solid boundary to a fluid flow field may drastically alter the action of the fluid upon a body immersed in it. Since an airplane operates in such a bounded region during landing and take off, the prediction of these changes in aerodynamic characteristics due to the ground is very important.

It has long been realized that a drag decrease and a stability increase may be expected due to the effect of the ground. Indeed, some of the early aircraft could not have flown had it not been for the aid of the ground effect. Considerable work, both theoretical and experimental, has been done on the problem of predicting ground effects. For unswept wings of normal aspect ratios the ground effects can be estimated with fair accuracy.

With the trend in modern day aircraft toward low aspect ratio, thin, swept wings, estimating the ground effect becomes difficult. In particular, the effects of sweep are not treated theoretically.

It is the purpose of this thesis to compare the effect of the ground on two low aspect ratio wings, one swept and one straight, and to attempt to calculate the changes due to the ground using available theory.

CHAPTER II
THEORETICAL ANALYSIS OF THE PROBLEM

Wieselsberger¹ in 1921 made an approximate analytical study of a wing flying close to the ground. Representing the ground by an image wing contained within the ground, he was able to calculate the change in induced drag and induced angle of attack on a wing with an elliptic load distribution using Prandtl's biplane interference theory.

Reid² and Wetmore³ performed full scale tests to determine the effect of the ground. Their data agreed with Wieselsberger's theoretical approach. Pistolesi⁴ summed up the available theory, and developed an approximation for the case of the infinite wing.

Tomotika^{5,6}, in 1933 and 1934, provided one of the first rigorous approaches to the problem. By the use of conformal transformations he was able to calculate the lift on a flat plate in a semi-infinite two dimensional stream.

Tomotika⁷ later extended his approach to the case where the trailing edge approached the ground, and in conjunction with Imai⁸ treated the case of an airfoil touching the ground with its trailing edge.

Tani and others⁹, utilizing a slightly different approach, extended the work to cover the case of a finite monoplane wing. The changes in angle of attack, drag, and pitching moment were developed. In this report and a later one¹⁰, they compare this theory with wind tunnel data for both finite and infinite wings, showing good qualitative

agreement.

The treatment by Tani is chosen for comparison with the experimental data, since it is the only one adapted to the three dimensional case. Some discrepancy is to be expected between this theory and the measured results, since this solution is somewhat in error for high angles of attack close to the ground⁹. The development of the theory is outlined below.

By representing an infinite wing with a thin airfoil by a vortex sheet, the ground can be replaced by another vortex sheet of equal but opposite sign, placed as far below the ground as the original wing is above the ground. This is the system of "real" and "image" wings. The vorticity distribution on the real wing is:

$$\gamma = a_0 \sqrt{\frac{1-\xi}{1+\xi}} + a_1 \sqrt{1-\xi^2} + a_2 \xi \sqrt{1-\xi^2} \quad (1)$$

where a_0 , a_1 , and a_2 are constants necessary to satisfy the boundary conditions of no flow normal to the airfoil at the airfoil.

The change in circulation about the real wing due to the image wing is equivalent to a change in the effective angle of attack. This change can be shown to be, approximately

$$\beta = a_0 \left[\frac{a_0}{2V \sin a_0} + \frac{a_1}{4V \sin a_0} - 1 \right] \quad (2)$$

where the constants must satisfy the boundary conditions for the real and image wing system.

The image wing with its equal and opposite circulation will change the velocity at the real wing. Concentrating the image sheet

vortex into a point vortex, the average change in velocity at the real wing can be shown to be

$$\frac{v}{V} = -\tau C_L \quad (3)$$

where

$$\tau = \frac{1}{8\pi} \frac{\frac{H}{c}}{\frac{H^2}{c^2} + \frac{1}{64}} \quad (4)$$

Hence, the effective velocity is $(1 - \tau C_L)V$.

Due to the blocking action of the finite thickness of the wing, the angle of zero lift will increase. Representing the real and image wings by appropriately placed doublets, it can be shown that the change in effective angle of attack is:

$$\Delta\alpha = -Ke \quad (5)$$

where e is the wing thickness expressed in chord lengths, and

$$K = 0.00300 \frac{H}{c} \left[\frac{1}{\left(\frac{H^2}{c^2} + \frac{1}{64}\right)^2} + \frac{3}{\left(\frac{H^2}{c^2} + \frac{9}{64}\right)} \right] \quad (6)$$

Using a lift curve slope of $2\pi n$, where n is an arbitrary reduction factor to account for the finite wing, and is taken to be $7/8$, the lift coefficient is:

$$C_L = 2\pi n (\alpha_0 + \beta - Ke) (1 - \tau C_L) \quad (7)$$

Substituting $\alpha_0 = C_L / 2\pi n$, α_0 being taken from the vortex distribution, the lift coefficient becomes, neglecting the product of small quantities

$$C_l = 2\pi n (a_0 + \beta - Ke - \frac{\tau C_l^2}{2\pi n}) \quad (8)$$

This corresponds to a change in effective angle of attack necessary to maintain a given lift coefficient of

$$\Delta\alpha = -\beta + Ke + \frac{\tau C_l^2}{2\pi n} \quad (9)$$

For computation purposes, the change in angle of attack is given by

$$\Delta\alpha = -B + Ke + TC_l^2 \quad (10)$$

The constants B, K, and T are tabulated in Ref. 9.

The change in pitching moment is considered in two parts; that due to the image wing, and that due to the blocking effect of the wing thickness. First, considering only the real and image vortex sheets, it can be shown that the moment about the leading edge in the presence of the ground is:

$$C_{m_{LE}} = \frac{1}{4} K_l + DC_l \quad (11)$$

where c_m is positive for nose down moments, and

$$D = \frac{1}{8} \frac{a_1 + a_2/2}{a_0 + a_1/2} \quad (12)$$

Considering the wing as replaced by an appropriate doublet, it

can be shown that the change in pitching moment due to thickness is:

$$\Delta C_{m_{LG}} = -Ee \quad (13)$$

where e is the wing thickness, and:

$$E = 0.0180 \frac{H}{c} \left[\frac{1}{\left(\frac{H^2}{c^2} + \frac{1}{64}\right)^2} + \frac{7}{\left(\frac{H^2}{c^2} + \frac{9}{64}\right)^2} \right] \quad (14)$$

Combining the two, the effect of the ground on the pitching moment is given by

$$\Delta C_{m_{LG}} = D C_L - Ee \quad (15)$$

The change in induced drag is given by:

$$\Delta C_{Di} = -\frac{\sigma}{\pi A} C_L^2 \quad (16)$$

and the change in effective angle of attack due to the trailing vortices is:

$$\Delta \alpha = -\frac{57.3 \sigma}{\pi A} C_L \quad (17)$$

where σ is Prandtl's biplane interference factor.

The preceding development was primarily two dimensional. Since the three dimensional case is extremely difficult, if not impossible, to handle analytically, a reduction factor, r , is used. This factor r is defined by

$$r = \frac{1}{2b} \int_{-b/2}^{b/2} (\cos \phi_1 + \cos \phi_2) dy \quad (18)$$

where the angles are defined as shown in Fig. 1 below

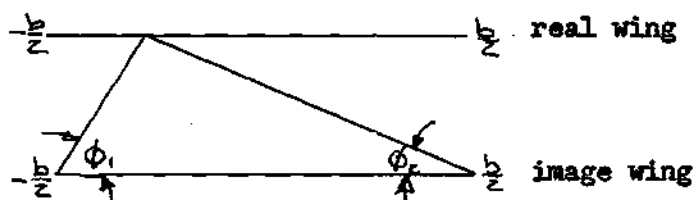


Fig. 1

Definition of Equation 18

Evaluating this integral there is obtained:

$$V = \sqrt{1 + \left(\frac{zH}{b}\right)^2} + \frac{zH}{b} \quad (19)$$

This reduction factor is applied to all quantities effected by the three dimensional character of the flow. These are the change in circulation, B; the change in longitudinal velocity, T; and the change in moment due to the image wing, D. Hence, summing all the changes, the final equations are

$$\Delta\alpha = -rB + Ke - \frac{57.3\sigma}{\pi A} C_L + rC_L^2 T \quad (20)$$

$$\Delta C_D = -\frac{\sigma}{\pi A} C_L^2 \quad (21)$$

$$\Delta C_{M_{LE}} = rDC_L - Ee \quad (22)$$

CHAPTER III
MODELS AND EQUIPMENT

Models-The two models used in this research project were built in the model shop of the Daniel Guggenheim School of Aeronautics. A tolerance of ± 0.02 inches was held. Both models were constructed of laminated mahogany with a polished lacquer finish. The tips of the delta wing were formed from aluminum.

Each wing was constructed to the NACA 0009 airfoil parallel to the plane of symmetry, and had an aspect ratio of 1.732. The basic span of each wing was 4.00 feet, with an area of 9.24 square feet for the delta, and an area of 9.54 square feet for the straight wing, including the wing tips. Each wing was designed so that the trunnion axis coincided with the quarter chord point of the MAC. The mounting holes were covered over during the testing so that minimum flow interference was obtained. The dimensions of the models are shown in Figs. 2 and 3 in the Appendix.

Tunnel-The nine foot wind tunnel of the Daniel Guggenheim School of Aeronautics was used to obtain all the test data. The test section is circular, of a constant nine foot diameter, with a length of twelve feet. The model was supported on a conventional three support system.

The forces on the model were measured by a six component electro-mechanical beam balance. This balance is capable of less than 0.10 per cent error when each component is loaded separately¹¹. The beam sensitivities are given in Ref. 11 as

lift = 0.10 lb.

drag = 0.05 lb.

pitching moment = 0.20 ft. lb.

Ground Planes-Three ground plane locations were used. These were termed high, mid, and low ground planes, referring to the height above the tunnel floor. Since both models have the same wing span, each model was tested at $\frac{2H}{b}$ ratios of 0.513, 1.025, and 1.540.

The ground planes were constructed of $\frac{3}{4}$ inch plywood. Each ground plane extended 1.45 chord lengths ahead of the mounting point, and 1.80 chord lengths behind. Streamlined supports were provided in the center of the tunnel while the edges were bolted to 2 x 2 aluminum angles fixed to the test section walls. These angles remained in place during all runs, but their effect was considered to be negligible. Fig. 4 shows the positions of the ground planes, while Figs. 5 and 6 show the models and ground planes installed.

CHAPTER IV

PROCEDURE

Prior to this test program the wind tunnel balance had been aligned and checked. The variation of dynamic pressure ("q") across the jet, and the variation of center line q with piezometer setting were available. This was for the unobstructed test section.

Due to the blocking effects, it was necessary to calibrate the piezometer ring, and to make q surveys for the three ground plane positions. For this purpose an eight foot pitot rake, employing nine pitot tubes on one foot centers, was used. Integration of the product of local chord times local q, all divided by the wing area, determined the mean q for each ground plane position. From this the ratio of mean q to center line q was obtained, assuming a linear variation of q with piezometer setting.

Wake and solid blocking corrections were obtained from Ref. 12. Knowing the blocking corrections, the variation of center line q with piezometer setting, and the ratio of mean q to center line q, the mean q over the wing may be set at any desired value. A nominal airspeed of 120 MPH, corresponding to a blocked q of 36.86 lb./ft.^2 , was used for all tests.

For each configuration, lift, drag, and pitching moments were measured through an angle of attack range from -6° to $+25^\circ$ on the delta wing, and to stall on the straight wing. The limit of 25° on the delta is due to interference between the model and the supports. Very little data was obtained beyond the stall for the straight wing because of the

extreme buffeting encountered.

For the free tunnel configuration, the wind tunnel data were corrected for alignment, tare and interference, and jet boundary effects. Alignment, tare, and interference corrections were obtained by normal wind tunnel procedures as outlined in Ref. 13. The jet boundary corrections were obtained from Ref. 14 for the straight wing, and Ref. 15 for the delta wing.

The ground plane wind tunnel data were corrected only for tare and interference. An attempt to use Ref. 16 to calculate the jet boundary corrections for the ground plane configurations was unsuccessful, since this report applies only to rectangular tunnels. The error introduced by neglecting this jet boundary correction is small¹⁶.

CHAPTER V

RESULTS

The results of the wind tunnel tests are presented in Figs. 7 through 12.

Delta Wing-The lift curve for the delta wing, Fig. 7, is linear only for small angles of attack. The non-linear range is due to the formation of a leading edge vortex caused by flow separation¹⁷. The extent of the linear range is proportional to the height above the ground plane, with the longest linear range occurring for the condition of no ground plane.

The normal effect of the ground is to cause an increase in lift curve slope, as is the case here. However, the further increase in slope due to earlier formation of the leading edge vortex adds to the ground effect, giving rise to changes not predicted by theory. A sizeable reduction in angle of attack necessary to produce a given C_L near the ground can be seen. For the high ground plane, at a C_L of 0.8 the angle of attack is only 83 per cent of the free flight value.

The drag polars for the delta wing are shown in Fig. 8. It can be seen that the drag decreases as the wing nears the ground, due to the restraining action of the ground planes. The reduction in drag for the high and mid ground planes is large. In the case of the high ground plane and a C_L of 0.8, the drag is only 72 per cent of the corresponding free flight drag.

For the low ground plane, only in the middle range of C_L 's is the effect beneficial. For C_L 's greater than 0.8 no distinction between the

low and no ground plane curves is apparent. The high and mid ground planes restrain both the downwash and the upwash around the wing. This restraining action then helps prevent tip stalling, and reduces the form drag. For the low ground plane, the restraining action of the ground planes is not great enough to prevent the stalling of the tips. Hence, any beneficial effects of the ground are masked by the increase in form drag.

The slope of the delta wing pitching moment curves, Fig. 9, is negative throughout the test range, indicating that this wing is stable about the quarter chord point of the MAC. As the delta wing approaches the ground the slope becomes more negative, representing an increase in stability. These moment curves are linear up to the point at which the leading edge vortex forms. As was the case for the lift curves, the linear range length is proportional to the height above the ground.

Straight Wing-Fig. 10 presents the lift curves for the straight wing.

These curves have the usual "hooked" shape of low aspect ratio straight wings¹⁸. The maximum lift coefficient attained was approximately 0.88 with no ground plane. However, due to the large turbulence factor of this tunnel, 1.37 from Ref. 19, no conclusions about the variation of $C_{L_{max}}$ with ground height could be drawn.

For all configurations the stall was sudden and complete. This is a combination of low aspect ratio and Reynolds number effect. As shown in TR 431²⁰, the low aspect ratio wing stalls suddenly. From Ref. 21 it can be seen that at the test Reynolds number this airfoil has a sudden stall which is not present at higher Reynolds numbers.

As before, the ground planes increase the slope of the lift

curves. However, the low and mid ground planes have only a slight influence. The high ground plane reduces considerably the angle of attack necessary to produce a given C_L . For a C_L of 0.8 in the presence of the high ground plane, the angle of attack is only 86 per cent of the free flight value. This reduction is not, however, as great as is the reduction for the delta wing. From above for the same conditions the angle of attack for the delta is only 83 per cent of the free flight value.

The straight wing drag polars are presented in Fig. 11. As in the case of the lift curves, only the high ground plane has an appreciable effect. For the high ground plane configuration and a C_L of 0.8, where the delta wing had only 72 per cent of the free flight drag, the straight wing has 82 per cent.

The moment data for the straight wing presented in Fig. 12 shows this wing to be unstable about the quarter chord point at low C_L 's and stable at high C_L 's. The aerodynamic center of the NACA 0009 airfoil is $0.250c^{21}$. Therefore, the pitching moments shown arise from the action of the trailing vortices on the wing. Due to the low aspect ratio this effect is considerable. The influence of the ground shifts the curves in the negative direction, the amount of shift increasing with C_L . Hence, like the delta wing, the straight wing becomes more stable in the presence of the ground.

Tuft Studies-Tuft studies of both models were made at the conclusion of the test program. At that time the delta wing had been modified for another test program by drilling mounting holes near the leading edges. These were not present during the force tests. As can be seen in the tuft photographs, Figs. 13 through 17, the trunnion mounting holes, and

the newly cut holes were faired over. Unfortunately, the small window size in the tunnel ceiling made it impossible to include all of either model in the photographs. The spanwise tuft spacings were 4 inches on the straight wing, and 2 inches on the delta wing.

For the delta wing the tuft studies were made with no ground plane installed. The first indication of a leading edge vortex is seen in Fig. 15, which corresponds to a C_L of 0.55. With increasing C_L the vortex is more clearly seen, indicating an increase in strength.

Stalling of the tips is also first seen in Fig. 15. The stalled region enlarges with increasing C_L , causing spanwise flow over a large portion of the wing.

The lower surface shows no discontinuous flow, except for the few tufts "captured" by the flow up and around the leading edge. Increasing spanwise flow can be seen with increasing C_L .

Tuft studies for the straight wing are shown in Figs. 18 through 21, with the high ground plane installed. Direct negative to negative comparison of similar photographs taken with the mid ground plane installed failed to show any noticeable change in flow pattern. Thus, these flow patterns represent the general case. These photographs show that increasing spanwise flow occurs with increasing C_L , due to the tip effects. With such a small aspect ratio a large percentage of the wing area is effected by this cross flow. Some separation occurs at 16° , but at the stall the entire flow separates, except for the extreme tips. As was pointed out above, this is a low aspect ratio and low Reynolds number effect.

The theory developed by Tani and others⁹ applies only to wings

with no sweep and normal aspect ratios. However, since no other extensive treatment of the three dimensional case is available, an attempt to calculate the incremental effects of the ground was made by using this theory. The theory applies directly to the straight wing, except for the effects of the very low aspect ratio. For a swept wing, such as the delta wing used here, an effective ground height must be defined. As the swept wing increases in angle of attack the tips and trailing edge approach the ground at a faster rate than for a straight wing. Hence, the height of the quarter chord point of the MAC is not indicative of the restraining action of the ground. In order to apply the theory a more representative height was defined by considering the inclination of the quarter chord line, the chord distribution, and the lift distribution.

Fig. 22 shows the theoretical lift distribution for the delta wing, as obtained from TR 921²². To aid in computation, and provide a finite lift coefficient at the tip, the approximating curve shown was used. Some error is introduced by using this free flight lift distribution, since the ground proximity will alter it.

The effective $\frac{c}{H}$ ratio was defined as

$$\left(\frac{c}{H}\right)_{\text{MEAN}} = \frac{1}{b_k} \int_{-b/2}^{b/2} \left(\frac{c}{H}\right) K \frac{C_L}{C} b_y \quad (23)$$

Thus a $\left(\frac{c}{H}\right)_{\text{mean}}$ will be defined for each angle of attack and each ground plane.

Figs. 23 through 25 present the incremental ground effect data, both measured and calculated, for the straight and delta wings. Fig. 26 presents experimental data from TN 2487²³ for a wing having a 40° swept

back quarter chord line, a taper ratio of 0.625, and an aspect ratio of 4.0. The calculated effects for this wing are also included.

Regarding the angle of attack, the theory is conservative for all three wings. For the delta, and the swept wing at a ground height of $0.513 b/2$, and a C_L of 0.8, the calculated angles of attack are 8.6 and 4.0 per cent respectively too large. For the 40° swept wing at a height of $0.468 b/2$ and a C_L of 0.8, the calculated value is 2.3 per cent too large.

For the drag, the straight wing calculations prove to be unconservative. Considering the same conditions as above the calculated drags of the straight, the delta, and the 40° swept wings are 98.5, 114.0, and 112.4 per cent of the measured values respectively.

The pitching moment calculations do not agree with the incremental measurements. For the previous conditions, the straight, the delta, and the 40° swept wings have calculated moments that are 315.0, 102.1, and 105.0 per cent of the measured quantities respectively.

On the basis of this analysis, the lift and drag on a straight wing of low aspect ratio in the presence of the ground can be predicted with a fair degree of accuracy. However, the pitching moment cannot be predicted within acceptable limits because of the influence of the trailing vortices on the wing.

The reverse is true for the two swept wings considered. In general the effective ground is much closer to a swept wing than a straight wing. This is a result of having the tips behind the point of rotation. Hence, a greater decrease in drag and angle of attack is realized.

The one major point of disagreement is in the change in the angle of zero lift, and the pitching moment at zero lift due to wing thickness. For the two wings considered here the theory predicts much larger changes than were measured. Ref. 23 points out that no appreciable change in angle of zero lift was measured.

To find the changes due to wing thickness the wings, real and image, were represented as two dimensional doublets. As the flow about low aspect ratio wings is more similar to the flow about a three dimensional doublet than a two dimensional one, this analysis leads to erroneous answers.

In conclusion, the theory provides acceptable preliminary data about lift and drag on a straight wing, but does not for a swept wing.

CHAPTER VI

CONCLUSIONS

(1) In the presence of the ground both a straight and a swept wing experience an increase in lift curve slope, a decrease in drag, and an increase in stability, due to the effect of the ground.

(2) The effect of the ground is greater on the swept wing than on the straight wing, due to sweep which brings the tips closer to the ground. The trailing edge is also much closer to the ground on a swept wing, due to the chord distribution. All this makes the effective ground appear closer to the wing.

(3) The ground effect on a straight wing can be predicted fairly well by the theory used herein. The effect of the ground proximity on a swept wing is not adequately predicted by this theory.

CHAPTER VII

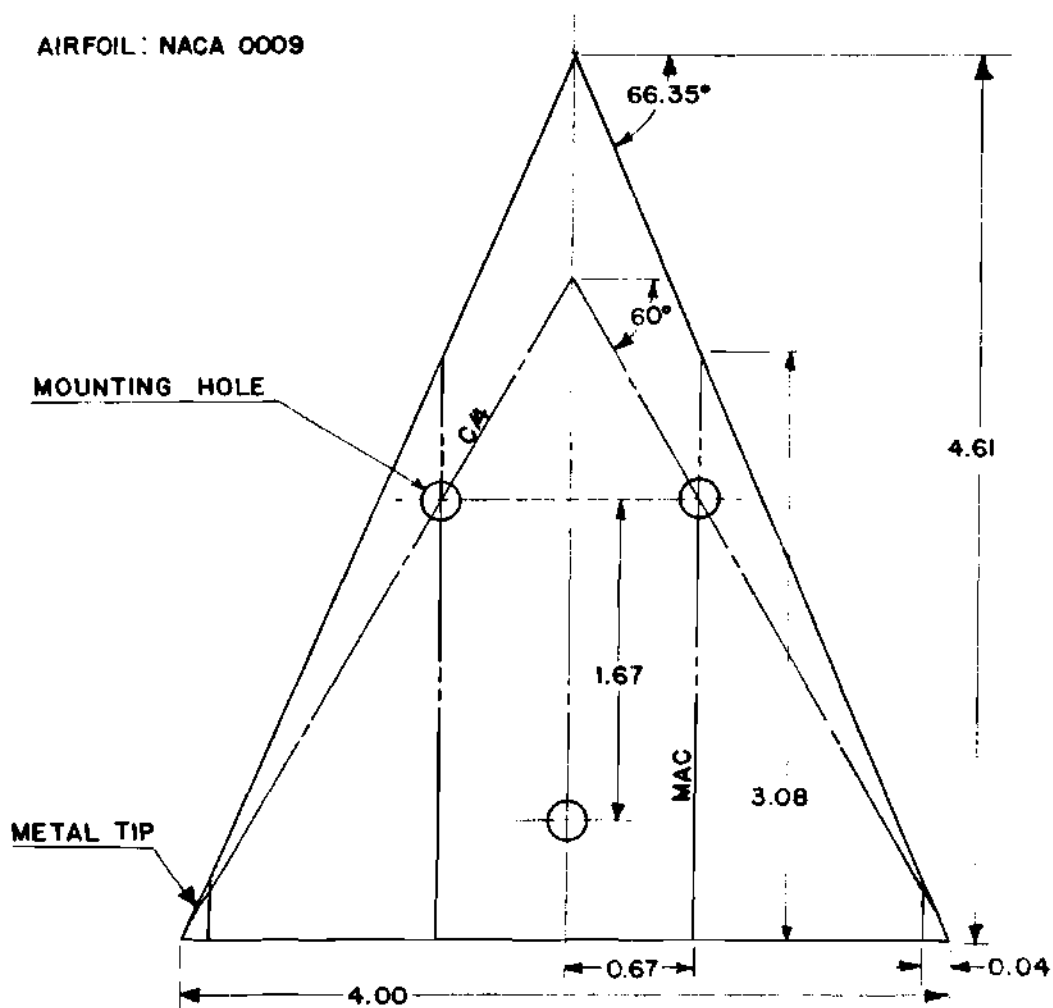
RECOMMENDATIONS

It is recommended that this experimental study be extended to cover other wings with various angles of sweep, and taper ratios. Testing should be done with more than three ground plane positions in order to accurately define the curves.

From the tests of the delta wing two interesting topics suggest themselves. First, the investigation of the influence of the tips on the characteristics of the wing. As the metal tips are detachable this study could be made quite easily. Secondly, the effect of the leading edge vortex on the characteristics of the delta. By the addition of a fairing with a sharp leading edge, a leading edge vortex can be generated over most of the lift range.

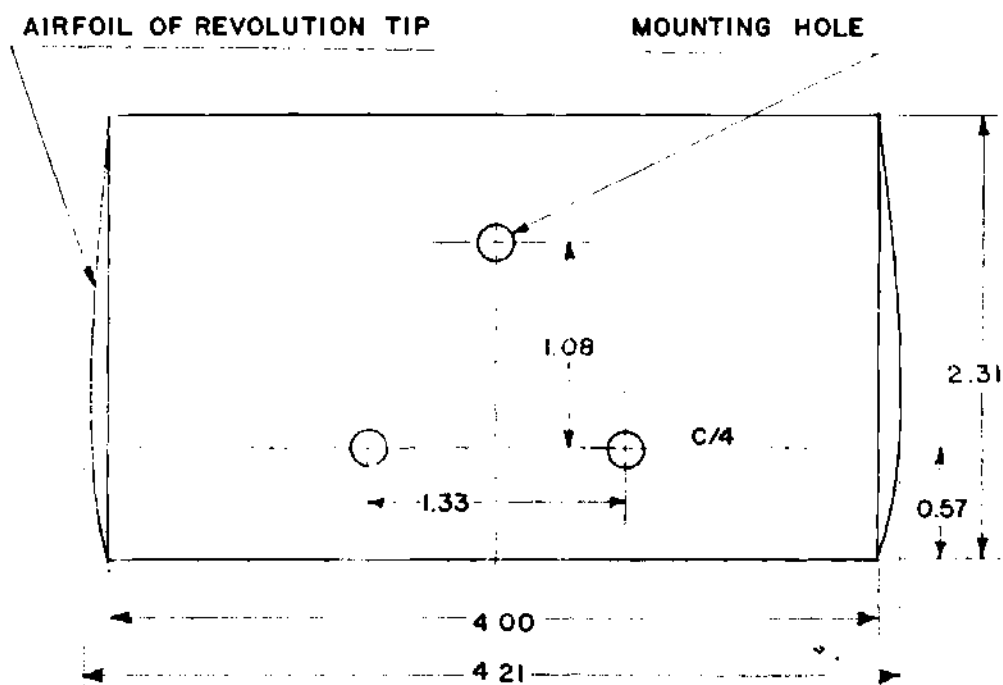
In the theoretical field, a more extensive treatment of the ground effect on a finite wing is desirable. Also, a more general treatment of the jet boundary corrections for ground effects is needed.

APPENDIX



ALL DIMENSIONS IN FEET EXCEPT AS NOTED

FIG. 2
 DIMENSIONS OF DELTA MODEL
 SCALE: 1" = 1'



AIRFOIL: NACA 0009

ALL DIMENSIONS IN FEET

FIG. 3
DIMENSIONS OF STRAIGHT WING MODEL
SCALE: 1" = 1'

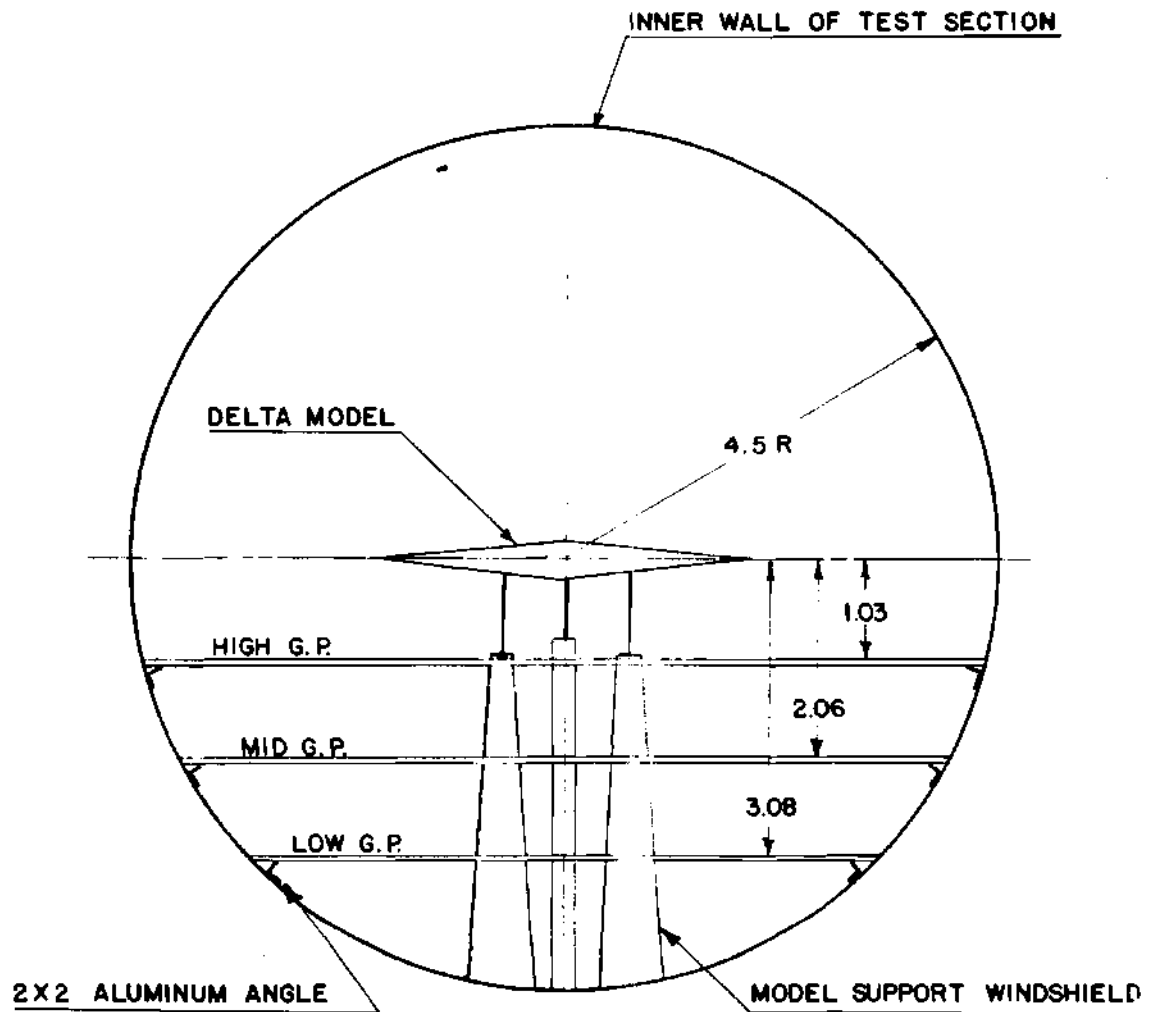


FIG. 4
GROUND PLANE POSITIONS
SCALE: 1/2" = 1'

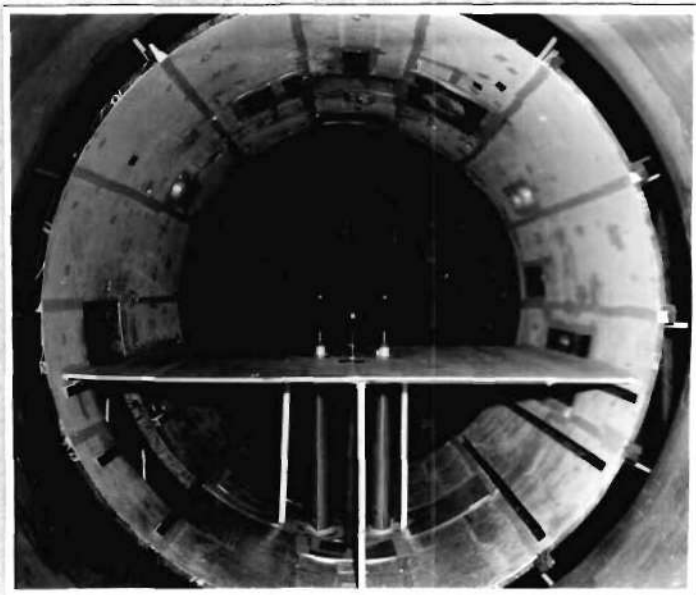


FIGURE 5
STRAIGHT WING AND HIGH GROUND PLANE.

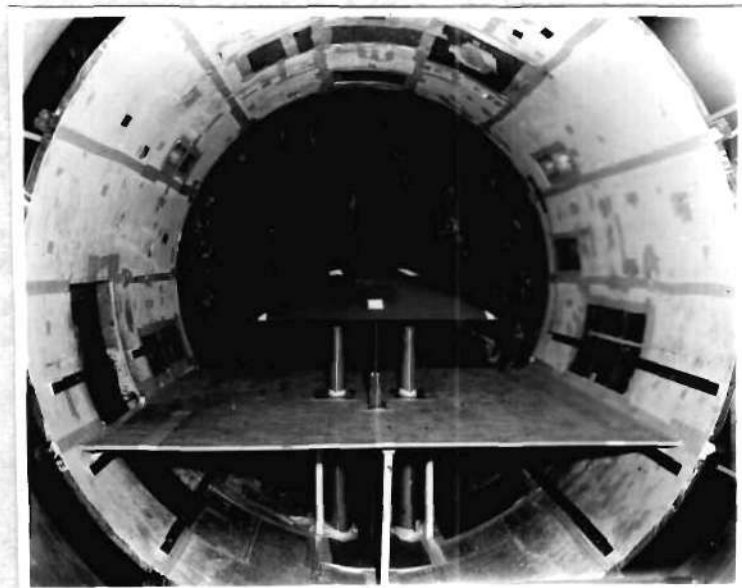


FIGURE 6
DELTA WING AND MID GROUND PLANE.

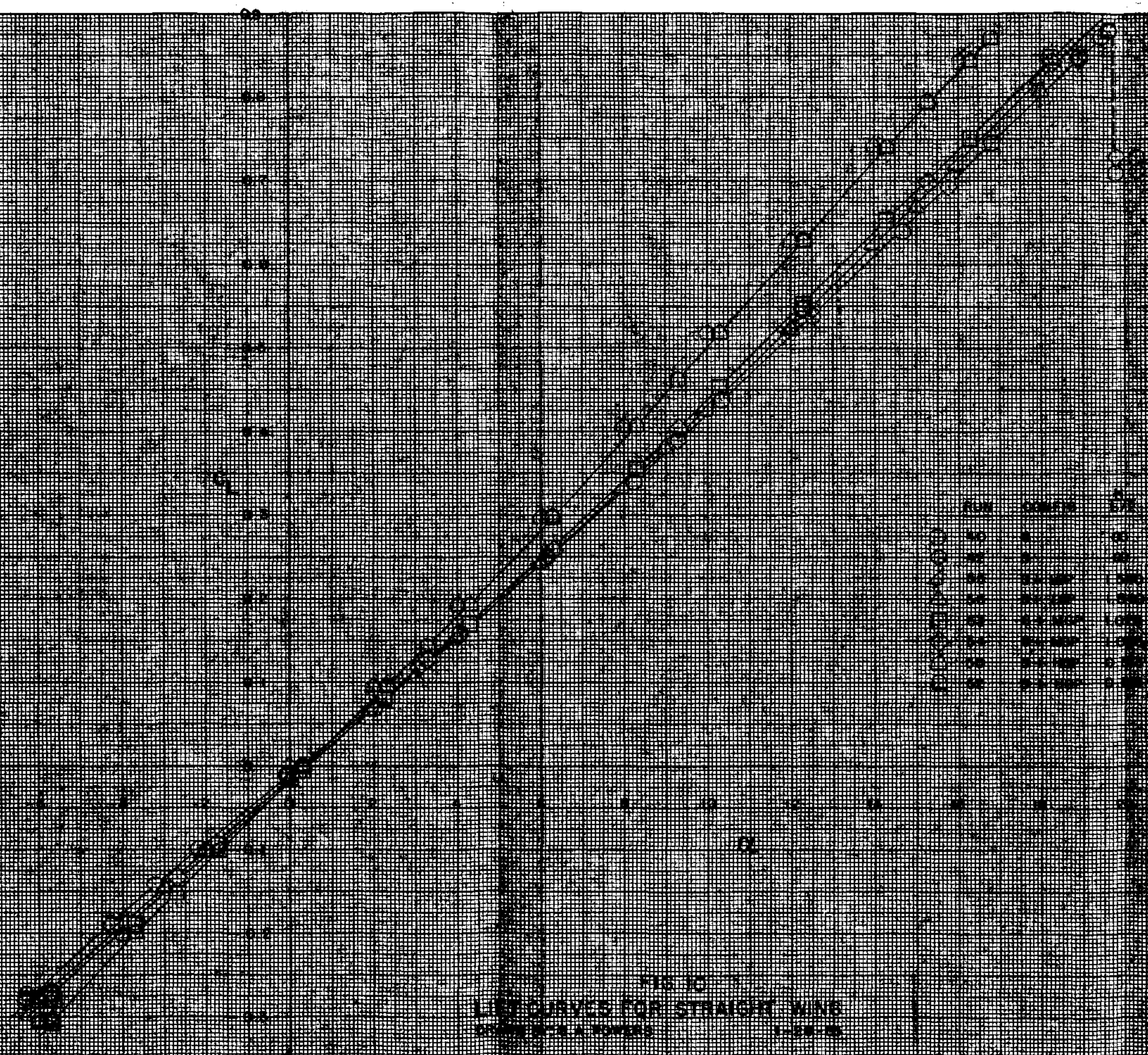


FIG. 10
 LIFE CURVES FOR STRAIGHT WINS
 (BASED ON A \$1000 INVESTMENT)

Days	Upper Curve (Dollars)	Lower Curve (Dollars)
0	100	100
10	150	140
20	220	200
30	320	280
40	450	380
50	620	500
60	850	650
70	1150	850
80	1550	1100
90	2050	1450
100	2650	1900

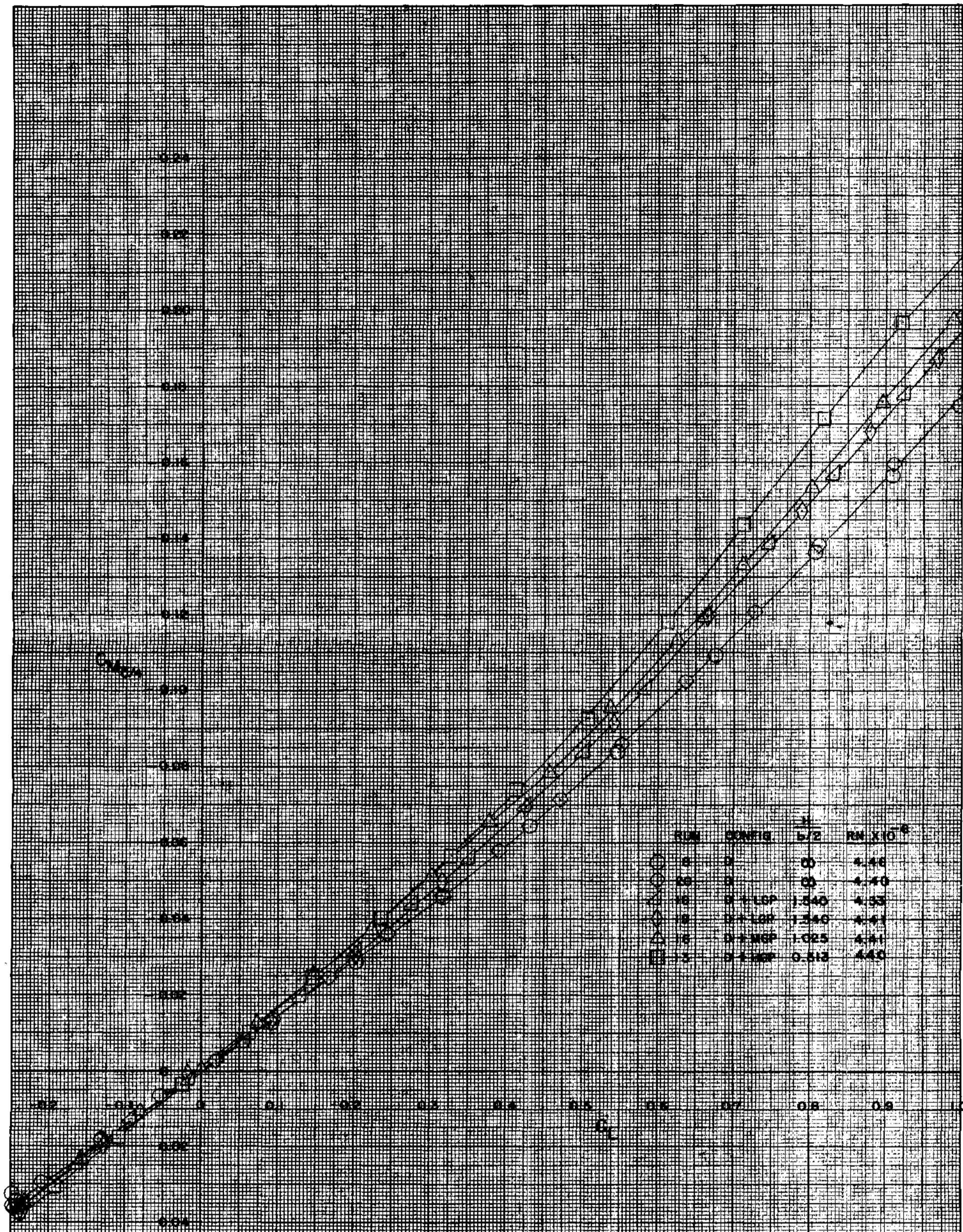
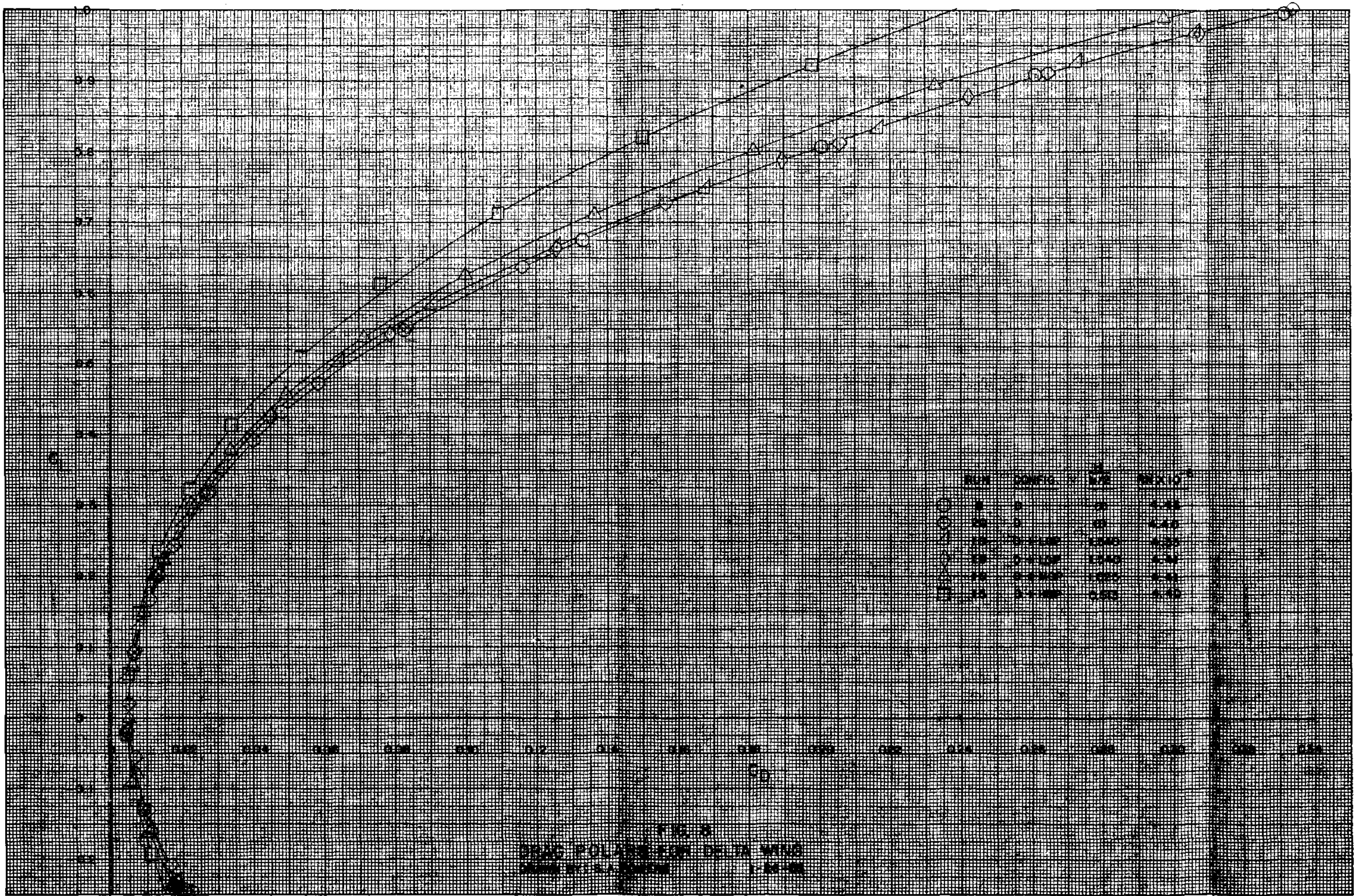


FIG. 2
 PITCHING MOMENT CURVES FOR DELTA WING
 DRAWN BY S. A. BOWEN 1-26-55



DRAG FORCE	VELOCITY	DRAG COEFFICIENT	ANGLE OF ATTACK
0.0	0.0	0.00	0.00
0.1	0.1	0.10	0.10
0.2	0.2	0.20	0.20
0.3	0.3	0.30	0.30
0.4	0.4	0.40	0.40
0.5	0.5	0.50	0.50
0.6	0.6	0.60	0.60
0.7	0.7	0.70	0.70
0.8	0.8	0.80	0.80
0.9	0.9	0.90	0.90

FIG. 3
 DRAG POLAR FOR DEUT. WING
 (DATA BY J. H. ...)

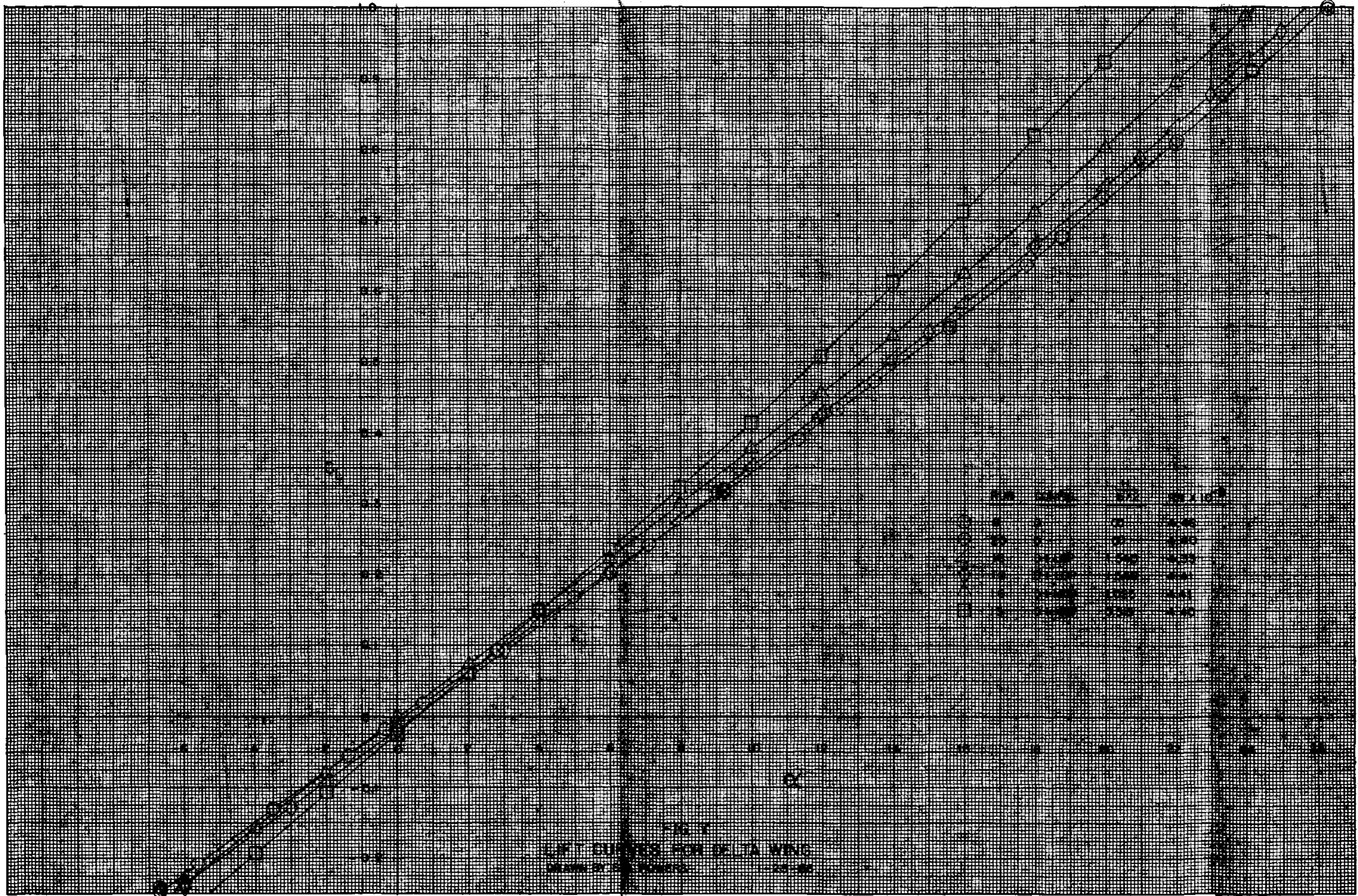
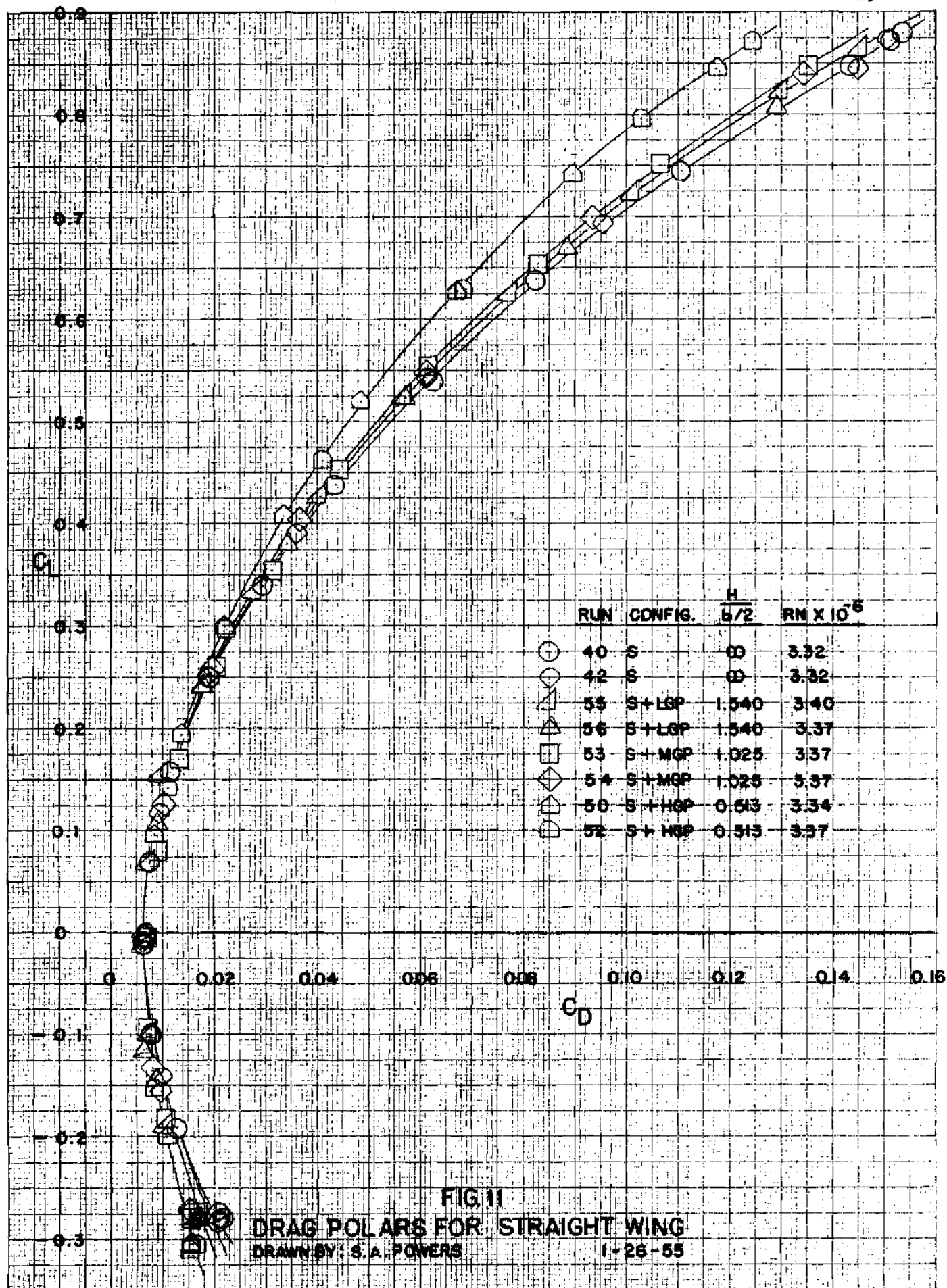


FIG. 1
LIFT CURVES FOR DELTA WING
MACH 0.2 TO 0.9



RUN	CONFIG	b/c	$Re \times 10^6$
40	S	00	3.32
42	S	00	3.32
55	S + LSP	1.540	3.40
58	S + LSP	1.540	3.37
53	S + MSP	1.025	3.37
54	S + MSP	1.025	3.37
50	S + MSP	0.513	3.34
52	S + MSP	0.513	3.37

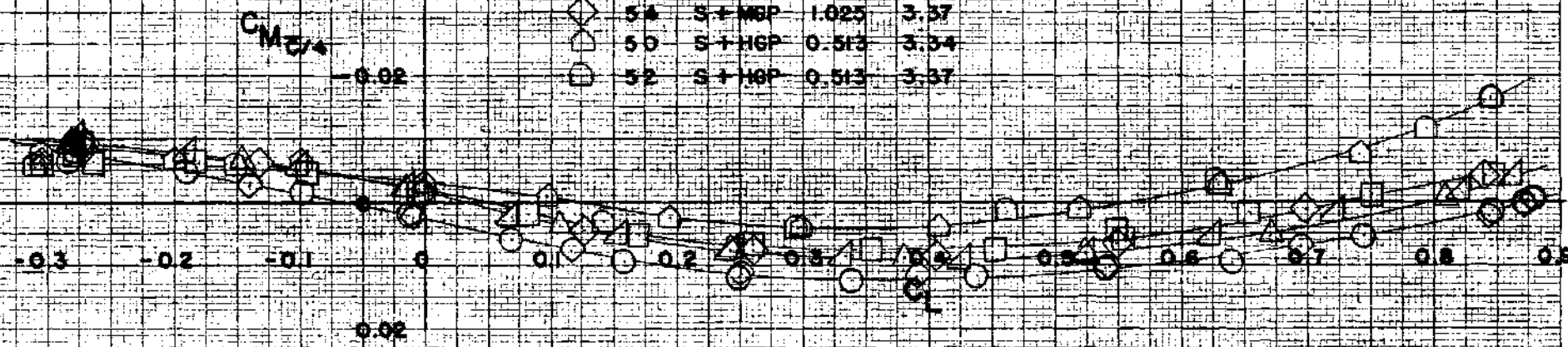
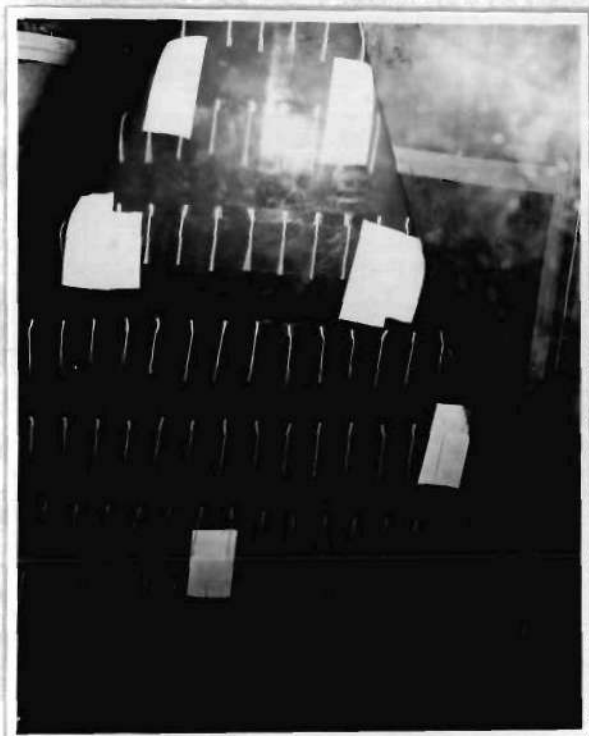
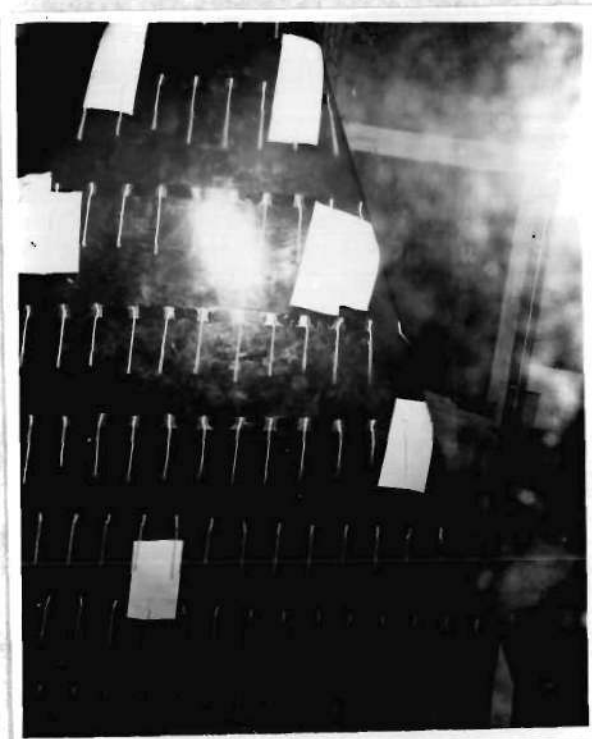


FIG. 12
 PITCHING MOMENT CURVES FOR STRAIGHT WING
 DRAWN BY: S. A. POWERS
 1-26-55



(a) UPPER SURFACE



(b) LOWER SURFACE

FIGURE 13
DELTA WING TUFT STUDIES
 $\alpha = 5.0^\circ$ $C_L = 0.17$

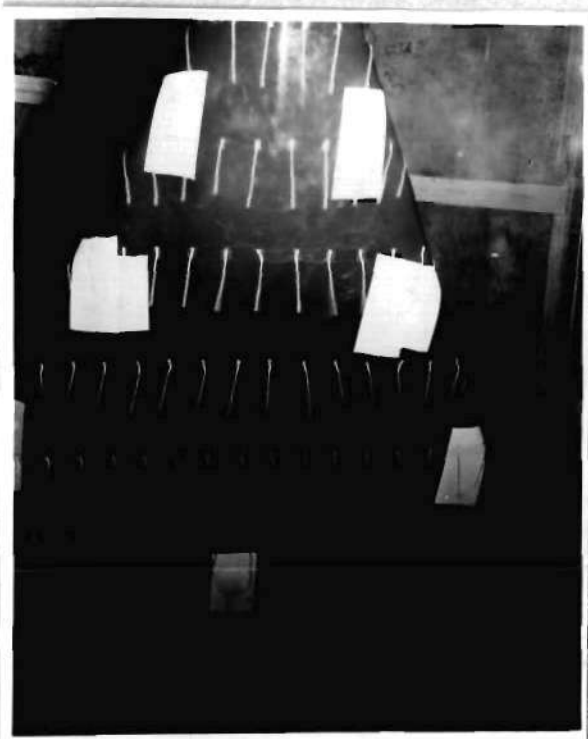


(a) UPPER SURFACE



(b) LOWER SURFACE

FIGURE 14
DELTA WING TUFT STUDIES
 $\alpha = 10.3^\circ$ $C_L = 0.35$

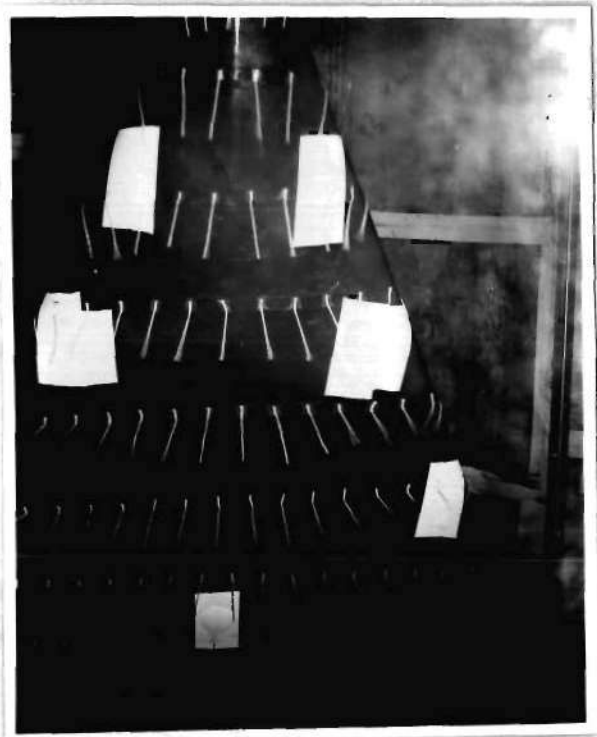


(a) UPPER SURFACE



(b) LOWER SURFACE

FIGURE 15
DELTA WING TUFT STUDIES
 $\alpha = 15.6^\circ$ $C_L = 0.55$



(a) UPPER SURFACE

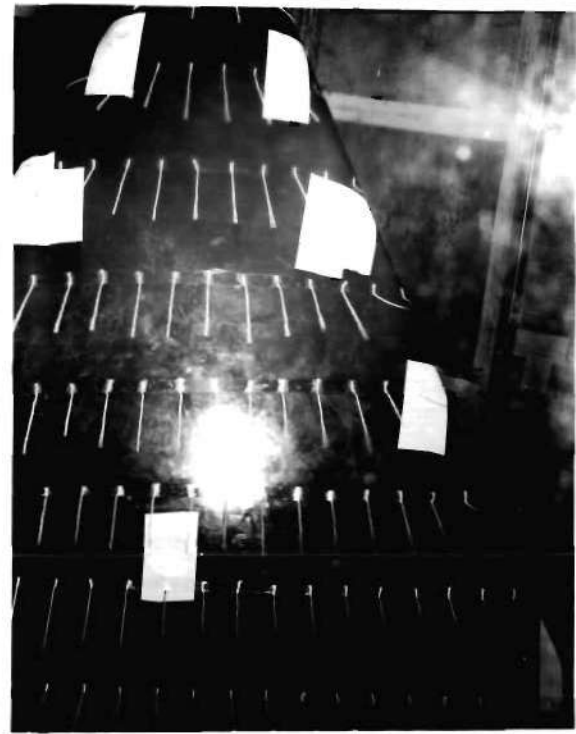


(b) LOWER SURFACE

FIGURE 16
DELTA WING TUFT STUDIES
 $\alpha = 21.0^\circ$ $C_L = 0.77$



(a) UPPER SURFACE



(b) LOWER SURFACE

FIGURE 17
DELTA WING TUFT STUDIES
 $\alpha = 26.3^\circ$ $C_L = 1.00$



$\alpha = 0^\circ$ $C_L = -0.01$

FIGURE 18



$\alpha = 8^\circ$ $C_L = 0.39$

FIGURE 19

STRAIGHT WING TUFT STUDIES
UPPER SURFACE



$\alpha = 16^\circ$ $C_L = 0.83$

FIGURE 20



$\alpha = 17^\circ$ $C_L = 0.78$

FIGURE 21

STRAIGHT WING TUFT STUDIES
UPPER SURFACE

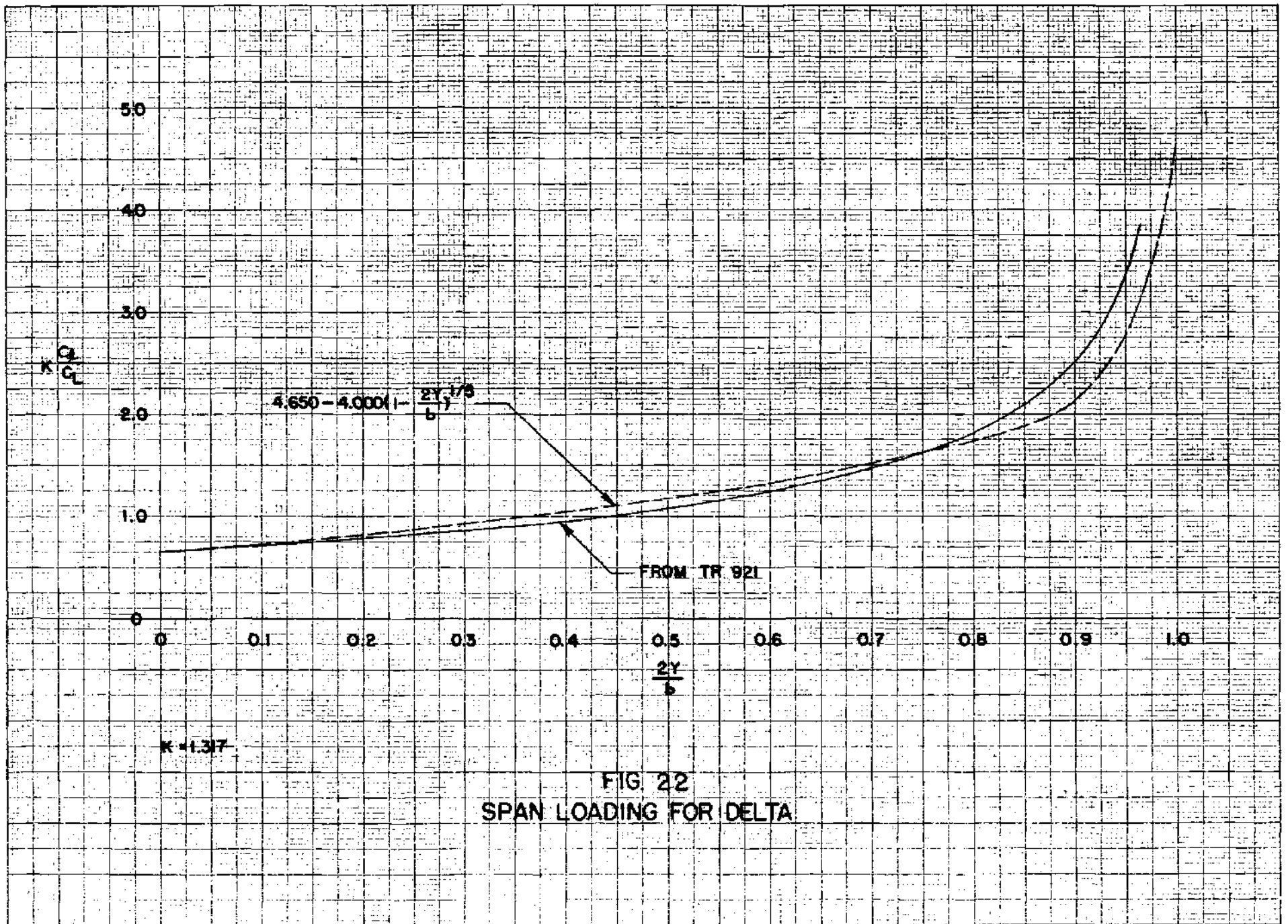


FIG. 22
SPAN LOADING FOR DELTA

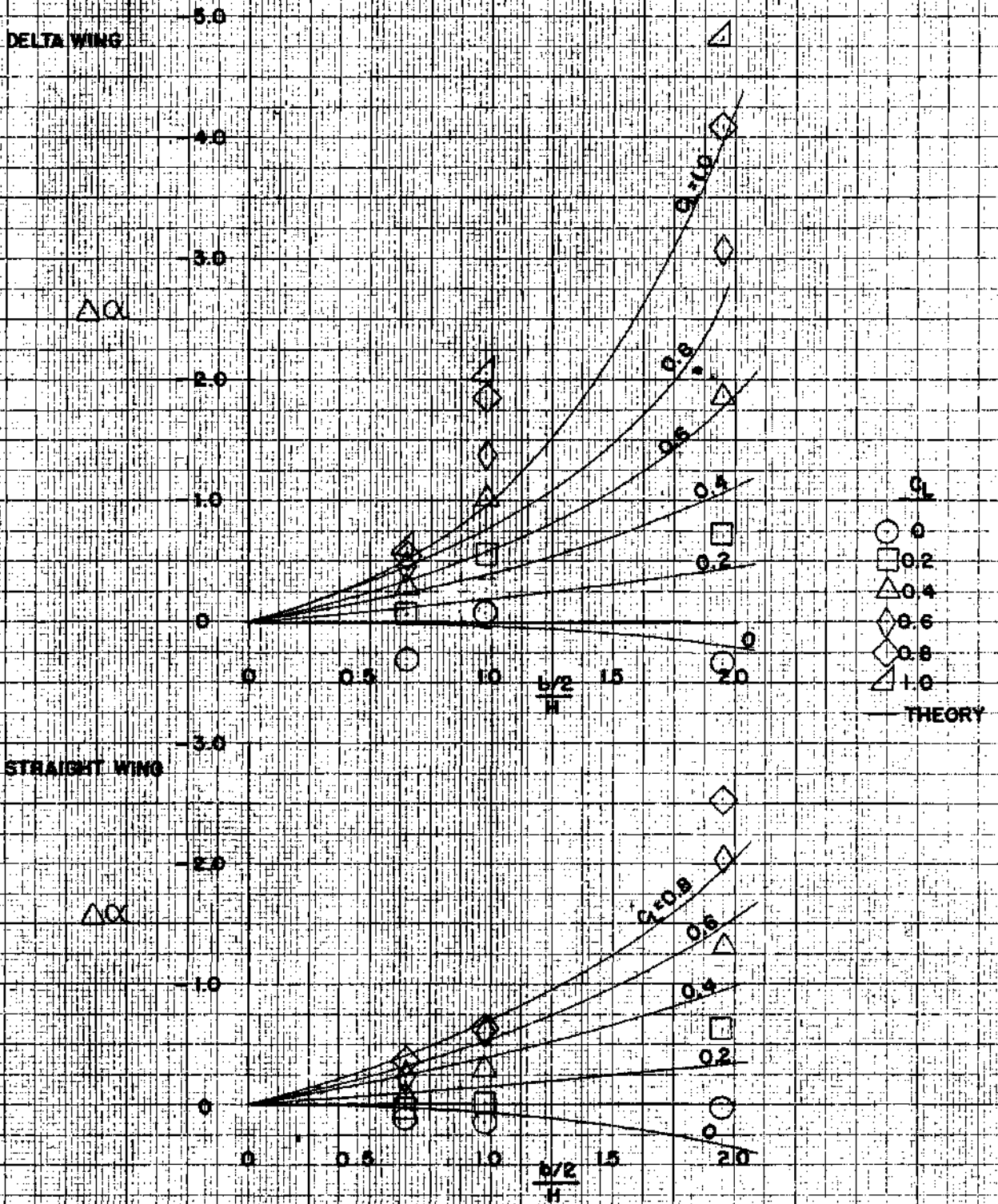


FIG. 23
 INCREMENTAL GROUND EFFECTS
 ANGLE OF ATTACK

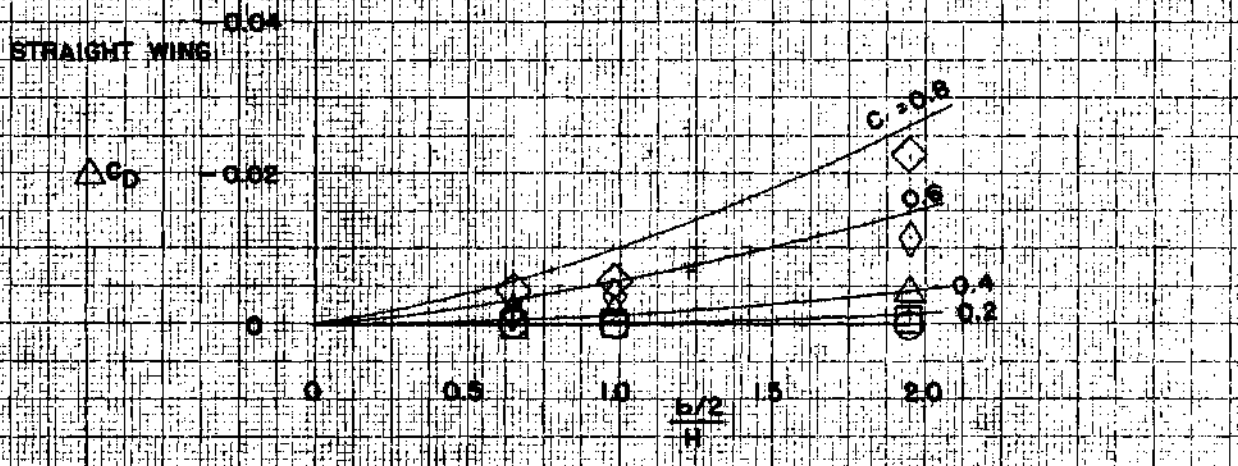
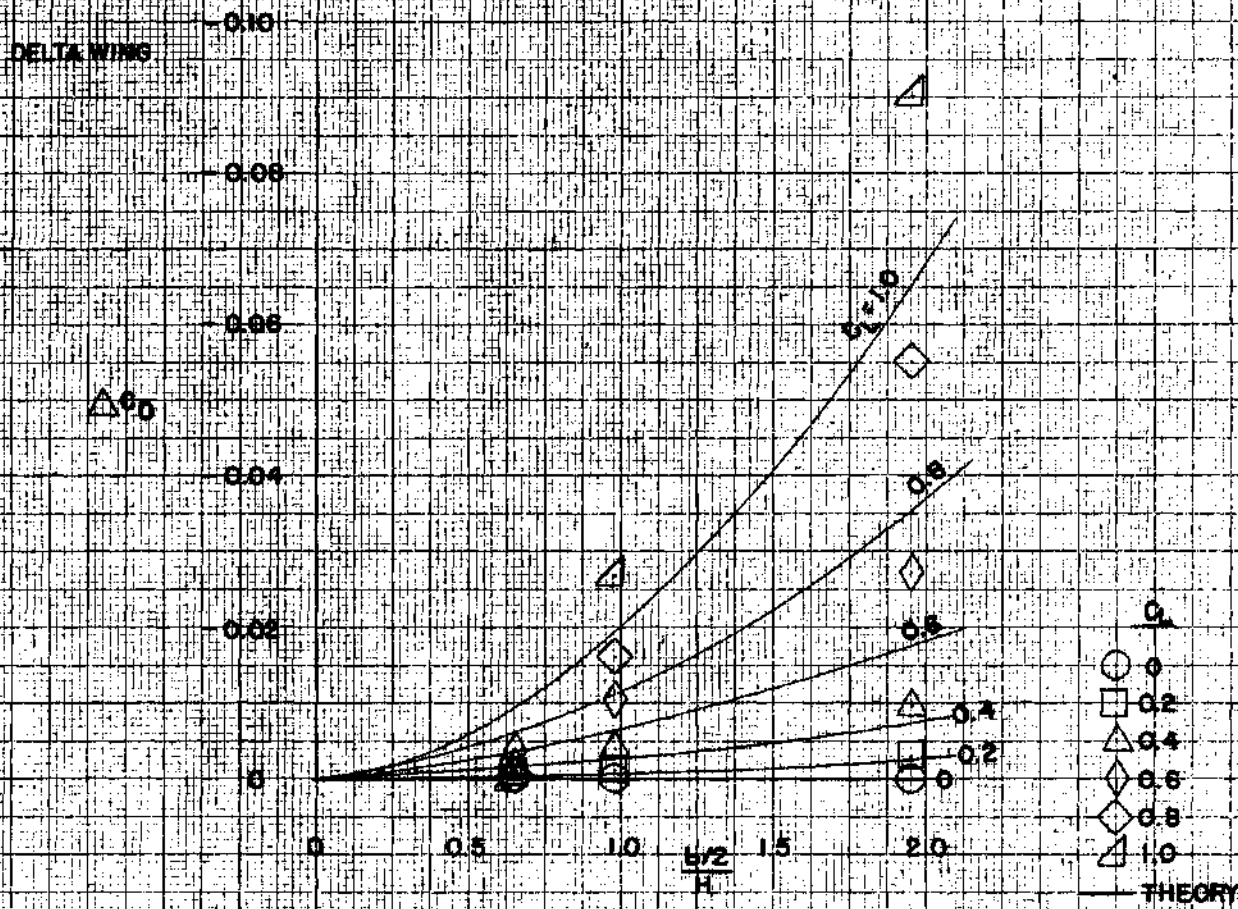


FIG. 24
 INCREMENTAL GROUND EFFECTS
 — DRAG —

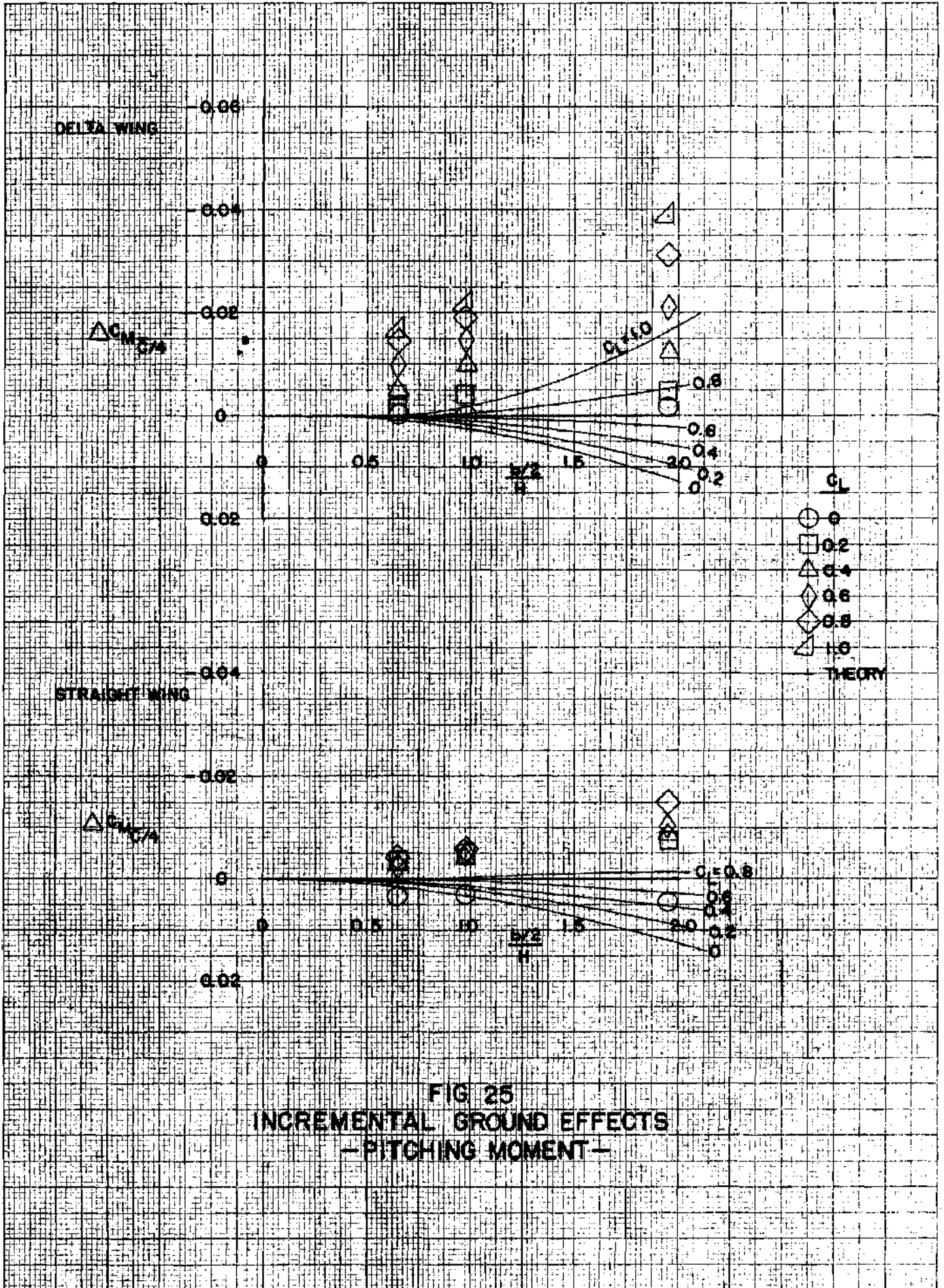


FIG 25
 INCREMENTAL GROUND EFFECTS
 - PITCHING MOMENT -

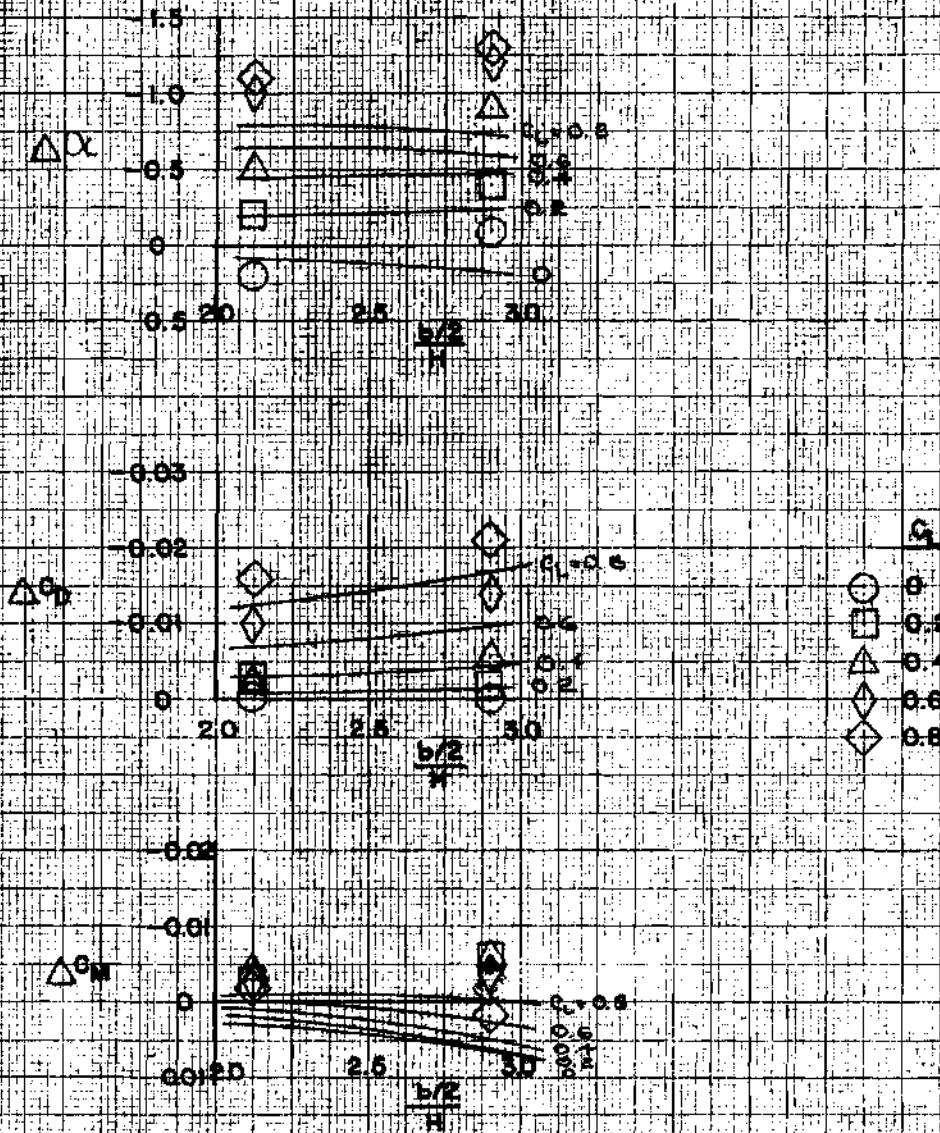


FIG. 26
 INCREMENTAL GROUND EFFECTS
 ON 40° SWEEP WING

BIBLIOGRAPHY

1. Wieselberger, C., Wing Resistance Near the Ground, National Advisory Committee for Aeronautics, Technical Memorandum No. 77, April, 1922.
2. Reid, R. G., A Full Scale Investigation of Ground Effect, National Advisory Committee for Aeronautics, Technical Report No. 265, 1927.
3. Wetmore, J. W., and Turner, L. T., Jr., Determination of Ground Effect from Tests of a Glider in Towed Flight, National Advisory Committee for Aeronautics, Technical Report No. 695, 1940.
4. Pistolesi, E., Ground Effect-Theory and Practice, National Advisory Committee for Aeronautics, Technical Memorandum No. 828, June, 1937.
5. Tomotika, Susumu and others, "The Lift on a Flat Plate Placed Near a Plane Wall, with Special Reference to the Effect of the Ground Upon the Lift of a Monoplane Aerofoil", Report of the Aeronautical Research Institute, Tokyo Imperial University, 8, No. 97, August, 1933.
6. Tomotika, Susumu, "The Lift on a Flat Plate Placed in a Stream Between Two Parallel Walls and Some Allied Problems", Report of the Aeronautical Research Institute, Tokyo Imperial University, 8, No. 101, January, 1934.
7. Tomotika, Susumu, "Further Studies on the Effect of the Ground Upon the Lift of a Monoplane Aerofoil", Report of the Aeronautical Research Institute, Tokyo Imperial University, 10, No. 120, April, 1935.
8. Tomotika, Susumu, and Imai, Isao, "Notes on the Lift and Moment of a Plane Aerofoil Which Touches the Ground with It's Trailing Edge", Report of the Aeronautical Research Institute, Tokyo Imperial University, 10, No. 126, May, 1935.
9. Tani, Itiro and others, "The Effect of Ground on the Aerodynamic Characteristics of a Monoplane Wing", Report of the Aeronautical Research Institute, Tokyo Imperial University, 13, No. 156, September, 1937.
10. Tani, Itiro and others, "Further Studies on the Ground Effect on a Aeroplane, with Special Reference to Tail Moment", Report of the Aeronautical Research Institute, Tokyo Imperial University, 13, No. 158, November, 1937.

11. Staff of Daniel Guggenheim School of Aeronautics, "The Georgia Tech Nine Foot Wind Tunnel", Brochure published by the Daniel Guggenheim School of Aeronautics, published prior to 1955.
12. Pope, A. Y., Wind Tunnel Testing, 2nd Edition, New York, John Wiley and Sons, 1954, p. 291.
13. Pope, Op. Cit., pp. 156-164.
14. Pope, Op. Cit., pp. 294-303.
15. Sivells, J. C., and Salmi, R. M., Jet-Boundary Corrections for Complete and Semispan Swept Wing Models in Closed Circular Tunnels, National Advisory Committee for Aeronautics, Technical Note No. 2454, 1951.
16. Brown, W. S., Wind Tunnel Corrections on Ground Effect, Aeronautical Research Council, Report and Memorandum, 1865, 1938.
17. Brown, C. E., and Michael, W. H., "Effect of Leading Edge Separation on the Lift of a Delta Wing", The Journal of the Aeronautical Sciences, 21, No. 10, October, 1954, p. 690.
18. Pope, Op. Cit., Fig. 5:55, p. 265.
19. Unpublished tunnel calibrations.
20. Zimmerman, C. H., Characteristics of Clark Y Airfoils of Small Aspect Ratios, National Advisory Committee for Aeronautics, Technical Report No. 431, 1932.
21. Abbott, Ira, H. and others, Summary of Airfoil Data, National Advisory Committee for Aeronautics, Technical Report No. 824, March, 1945, p. 132.
22. DeYoung, J., and Harper, C. W., Theoretical Symmetric Span Loadings Subsonic Speeds for Wings Having Arbitrary Plan Form, National Committee for Aeronautics, Technical Report No. 921, 1948.
23. Furlong, G. C., and Bollech, T. V., The Effect of the Ground Interference on the Aerodynamic Characteristics of a 42° Swept-Back Wing, National Advisory Committee for Aeronautics, Technical Note No. 2487, October, 1951.